

# PHOTOLUMINESCENCE-BASED CURRENT-VOLTAGE CHARACTERISATION OF INDIVIDUAL SUBCELLS IN MULTI-JUNCTION DEVICES

Diego Alonso-Álvarez<sup>\*1</sup>, David Lackner<sup>2</sup>, Simon P. Philips<sup>2</sup>, Andreas W. Bett<sup>2</sup> and Nicholas Ekins-Daukes<sup>1</sup>

<sup>1</sup>Imperial College London, London, United Kingdom

<sup>2</sup>Fraunhofer Institute for Solar Energy Systems ISE in Freiburg, Germany

\*Phone: +44 (0) 20 7594 7563, e-mail: [d.alonso-alvarez@imperial.ac.uk](mailto:d.alonso-alvarez@imperial.ac.uk)

**ABSTRACT:** In this work we develop a photoluminescence based, contactless method to determine the current-voltage characteristics of the individual subcells in a multi-junction solar cell. The method, that expands known results for single junction devices, relies on the reciprocity relation between the absorption and emission properties on a solar cell. Laser light with a suitable energy is used to excite carriers selectively in one junction and the internal voltages are deduced from the intensity of the resulting luminescence. The IV curves obtained this way on 1J, 2J and 6J devices are compared to those found using electroluminescence, finding good agreement between both at high injection conditions and attributing the discrepancies at low injection to in-plane carrier transport.

**Keywords:** III-V semiconductors, solar cell, characterization, photoluminescence

## 1 INTRODUCTION

Rapid growth of photovoltaic industry requires the development of fast and reliable tools for solar cell characterization. Evaluation of material and device properties using such techniques is critical for the study of fundamental solar cell physics, determining ways of improving device performance and optimizing the fabrication technologies. This is especially important for III-V multi-junction (MJ) solar cells that need to further reduce fabrication costs and increase efficiencies in order to see a higher penetration in the PV market.

In this work we develop a photoluminescence-based contactless method for current voltage (IV) characterization of MJ solar cells. Laser light is employed for carrier photogeneration in individual component junctions and free energy of the electron-hole pairs is measured from a photoluminescence (PL) signal. While this technique has been used for characterising single junction devices [1],[2], its extension to MJ devices has been limited, despite the remarkable opportunity it offers. The advantages of the method include:

- independent biasing of component junctions in a multi-junction solar cell for estimation of IV curves of each of the sub-cells;
- no necessity in taking into account series resistance;
- compatibility with both completed and partially finished solar cells. The method can be performed at every stage of the device fabrication – for example after the fabrication of each subcell - and used for monitoring and improving the manufacturing steps.

The PL-based IVs will be compared with the results obtained from electroluminescence (EL) experiments. EL has been used for characterising the internal voltages of MJ solar cells with excellent results [3], being the main disadvantage that it can only be applied on completely finished devices.

## 2 THEORETICAL BACKGROUND

The luminescence (photon flux) of a solar cell  $\phi_{em}$  and their external quantum efficiency  $Q_e$  are related by the spectral reciprocity relation, given by [3]:

$$\phi_{em}(E) = Q_e(E)\phi_{bb}(E) \left[ \exp\left(\frac{qV}{kT}\right) - 1 \right], \quad [1]$$

with  $\phi_{bb}$  the emission of a black body,  $V$  the internal voltage of the cell, equal to the quasi-Fermi level separation, and  $V_T = kT/q$  the thermal voltage. Considering that the luminescence is given in arbitrary units and using the Boltzmann approximation, the internal voltage  $V_j$  of a particular junction  $j$  in a MJ solar cell can be written as:

$$V_j = V_T \ln(\phi_{em}^j) + \frac{E}{q} - 2V_T \ln(E) - V_T \ln(Q_e^j) - C, \quad [2]$$

with  $C$  a constant that is determined during the calibration. In EL-based IV, the injected current density  $J_{inj}$  is given by the electrically injected current divided by the area of the device – usually defined by an etched mesa. In PL-based IV,  $J_{inj}$  is given by:

$$J_{inj} = J_{ex} = \frac{qP_{ex}Q_e(E_{ex})}{E_{ex}A_{ex}} \quad [3]$$

where  $P_{ex}$  is the laser power,  $E_{ex}$  the energy per photon, and  $A_{ex}$  the area of the excitation spot. This equation assumes that all photogenerated carriers contribute to the internal voltage of the cell in the  $A_{ex}$  area,  $J_{inj} = J_{ex}$ . As we will see below, this assumption is incorrect at low injection levels.

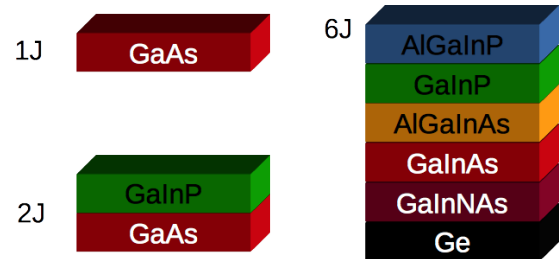


**Figure 1:** Structure of the solar cells used in this work [4].

## 3 EXPERIMENT AND MATERIALS

### 3.1 Solar Cells

We analyze three solar cells with 1, 2 and 6 junctions. The 1J device, made of GaAs was used to calibrate the setup – find out the value of  $C$  in Eq. 2. The 2J device is made of GaInP/GaAs whereas the 6J device is a structure

involving a dilute nitride 1 eV subcell lattice matched to Ge (see Fig. 1) [4]. The structures were processed in the form of devices with a dense front metal grid suitable for concentration/high injection measurements.

### 3.2 Experimental setup

EL and PL measurements shared the same collection optics: a doublet of lenses collected the light emitted by the samples and focused it into an optic fiber tip. The relation of the focal lengths of the lenses and the size of the core of the fiber gave a circular collection area 650  $\mu\text{m}$  in diameter. The fiber was connected to a fast Ocean Optics HR4000 spectrometer for measuring emission between 300 and 1000 nm, or to a grating spectrometer with an un-cooled InGaAs detector at the output for emission between 1000 nm and 1800 nm. A halogen lamp with known spectral shape was used to correct the measurements for the spectral response of the system.

Samples were positioned such that the collection spot was centered in the device. For PL experiments, a Nd:YAC laser or a tunable Ti:Sapphire laser were used. The excitation spot was oval, 1200x1450  $\mu\text{m}$ , completely covering the collection region with homogeneous illumination. The geometry and position of the sample was kept constant between measurements, ensuring that the same region is probed in both EL and PL experiments and that the calibration is also common.

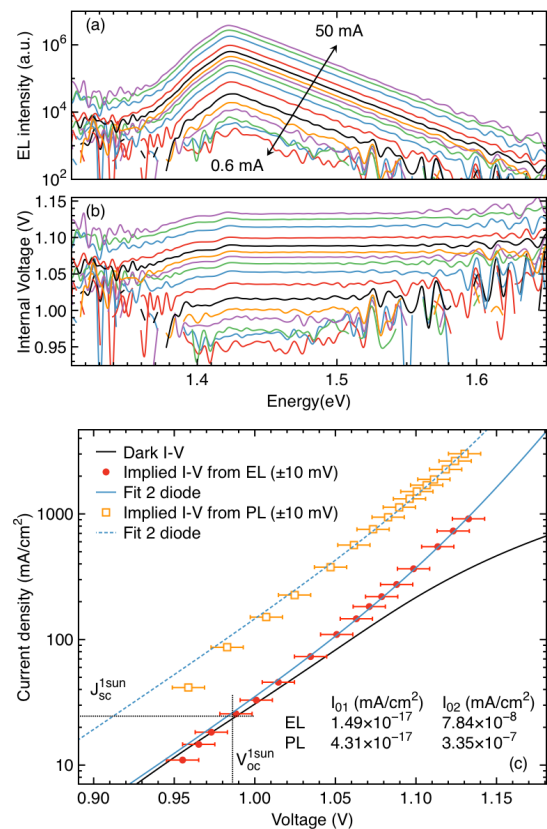
QE measurements were taken using a spot size for the monochromatic light also of  $\sim 650$  nm and probing the same region of the solar cell than in EL/PL experiments. This QE is influenced by the shadowing of the metal grid present in that region, which is important in order to have a common correction factor  $C$  for all samples, regardless of the exact metal grid design.

## 4 EXPERIMENTAL RESULTS

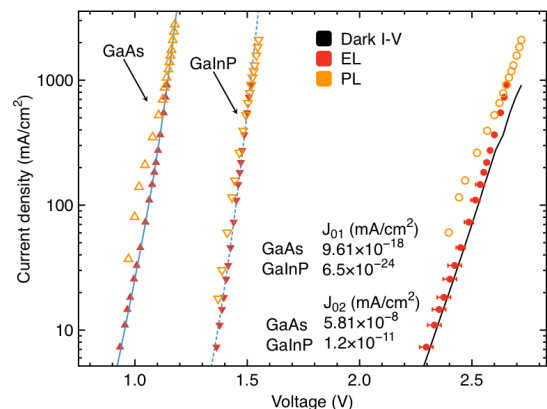
### 4.1 Calibration

Fig. 2 shows the EL spectra of the 1J GaAs sample as a function of the injected current, from 0.6 mA to 50 mA, and the calculated internal voltage using Eq. 2. This equation requires to know  $C$ . The procedure to obtain its value is as described in [3]: the voltages are calculated ignoring that constant and then they are shifted such that at a current equal to the short circuit current at 1 Sun, the voltage is equal to the corresponding open circuit voltage. Fig. 2c shows the resulting EL-based IV curve and the comparison with the measured dark IV of the device. As it can be seen, the agreement between both curves is very good at low injection levels. At higher levels, the normal dark IV becomes affected by series resistance while the the EL-based IV, free of series resistance, follows the usual shape that can be fitted with a two diode model.

Fig. 2c also shows the IV curve calculated from PL measurements (730 nm excitation, from 1.1 mW to 80 mW) using the same calibration factor that for EL. While the voltages are roughly the same – as expected considering that the EL and PL spectra almost overlap each other in this current and laser power range – currents appear to be overestimated. We will return to this discrepancy below.



**Figure 2:** (a) EL emission from the 1J GaAs sample. (b) Calculated internal voltages, including the correction factor, as a function of energy, fairly constant over the high energy side of the EL peak. (c) Implied IV curves from EL and PL measurements, fitting to a two diode model and comparison to the normal dark IV curve.



**Figure 3:** Implied IV curves from EL and PL of the 2J solar cell, as well as the total IV curves and the dark IV. The values of  $J_{01}$  and  $J_{02}$  are the result of fitting the implied IV curves from EL to a 2-diode model.

### 4.2 2J GaInP/GaAs solar cell

The same experiments were conducted on the 2J device using a 532 nm laser for the GaInP subcell and a 730 nm laser for the bottom one. The power range was the same in both cases, from 1.1 mW to 80 mW. The correction factor  $C$  is the one obtained previously.

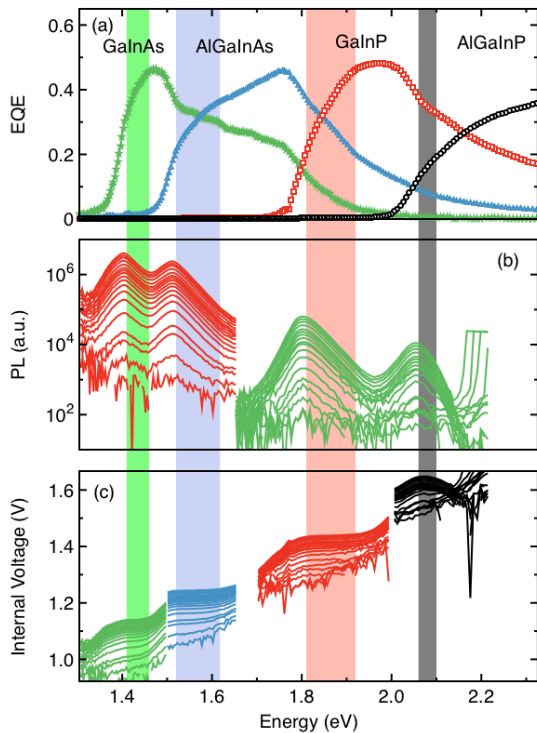
Fig. 3 shows the resulting IV curves for each subcell and the total IV curve calculated by adding together the

voltages at a given current. The EL-based IV curve of both junctions follow a 2-diode model accurately and the total IV is very similar to the dark IV at low injection, diverging just at higher values when the latter is influenced by series resistance. As with the 1J, the PL-based IV are above those from EL at low injection, getting closer and overlapping at high injection. For the case of GaInP, this effect is less marked, although at high injection the trend of the curves suggests that the results from PL will be *below* those from EL.

#### 4.3 6J solar cell

For the 6J solar cell we used the same two excitation wavelengths, 532 nm and 730 nm, in order to excite luminescence in the top (AlGaInP and GaInP) and the middle (AlGaInAs and GaInAs) two subcells, respectively (Fig. 4b). The reason is the strong overlap between the QE of these cells, as it can be seen in Fig. 4a, making very difficult to excite just one subcell. This might represent a problem just at very high injection levels when luminescence coupling between subcells becomes a relevant fraction of the total injected current.

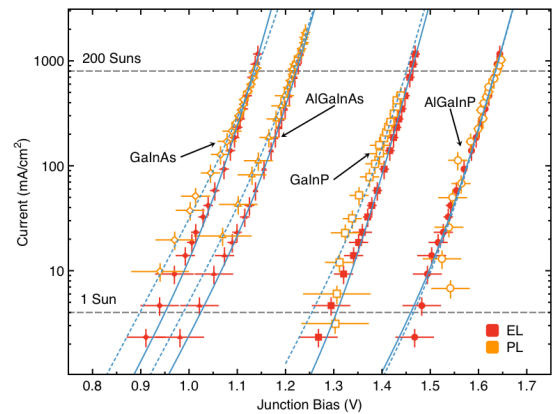
Regretfully, emission from the bottom subcells (GaInAs and Ge) could not be measured, probably because a combination of reduced luminescence and low sensitivity of our setup in this spectral region. As a consequence, the total IV curve could not be compared to the dark IV to support the validity of the model.



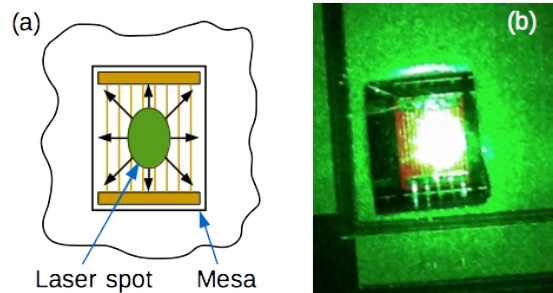
**Figure 4:** (a) External QE of the top and middle subcells of the 6J device. (b) PL emission when excited with the two lasers as a function of power. (c) Calculated internal voltages for each cell. The vertical colour bands indicate the regions that are averaged in each case to calculate the voltages and their uncertainties.

Fig. 5 shows the EL- and PL-based IV curves. They follow the same trend already discussed in the 1J and 2J solar cells, with the PL-based IV laying above the EL-based

one. However, here it becomes clearer that both curves tend to the same values at high injection.



**Figure 5:** Implied IV curves from EL and PL for the top and middle junctions of the 6J solar cell. Blue lines indicate fits to a 2-diode model in each case.



**Figure 6:** (a) Carriers photogenerated in the region of the laser spot travel in the plane of the sample and recombine in the whole mesa. (b) Picture of one of the devices, showing the bright green spot of the laser in the middle and red PL coming from the regions around.

## 5 DISCUSSION

### 5.1 The role of in-plane transport

Despite the agreement of voltages in all cases, it is clear that there is a discrepancy in the estimation of the current density when using EL and PL, specially at low injection levels. Such discrepancy was already outlined in Section 2 when we introduced Eq. 3: not all photogenerated carriers recombine in the region where they are generated; an important fraction is transported laterally, further if the material has high conductivity, until reaching the end of the mesa (Fig. 6a). As a consequence, although generation takes place in the excitation oval described before, recombination takes place everywhere in the device. This can be clearly seen in Fig. 6b where the bright, green spot of the laser in the centre of the sample is surrounded by red PL emission from the GaInP subcell coming out from the whole device.

To prove this point, we have carried out a simple calculation, modelling the in-plane transport with a 1D-mesh of resistances and the solar cells as diodes. This model is used often with several degrees of sophistication to estimate the dark currents and sheet resistance of silicon solar cells using EL imaging [5]. Fig. 7a shows a schematic representation of the model. Light is optically

injected in the central nodes of the 1D circuit. Ideally, that photogenerated current should flow through the diodes of those nodes but in practice, some of it will flow away, towards the nodes in the dark.

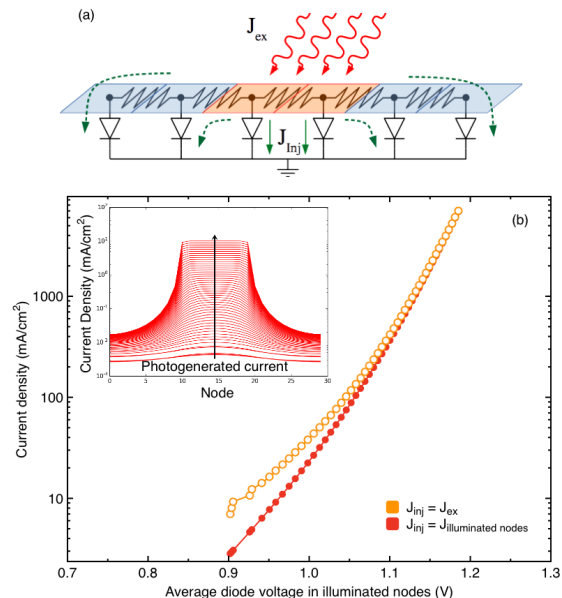


**Figure 7:** (a) Schematic representation of the 1D model for in-plane transport. Orange region represent the illuminated nodes. (b) Simulated IV curves for the two assumptions about the injection current. The inset shows the current flowing across each diode as a function of the photogenerated current.

Fig. 7b shows the resulting IV curves using some sensible, but arbitrary, values for the saturation currents – using a 2-diode model – and the resistors. At low injection, a large fraction of the photogenerated current will flow to adjacent nodes, therefore reducing the amount that is actually injected in the illuminated nodes. As the injection increases, more current will flow to the adjacent nodes, increasing the voltage drop across the resistors and biasing the diodes of the illuminated region, making them more conductive. Overall, the current flowing away represent a smaller fraction that the photogenerated one, making the two IV curves to get closer. Ultimately, virtually all photogenerated current will flow through the illuminated nodes.

High in-plane conductivity of the material – meaning low resistance in the model – will lead to a larger discrepancy between both curves. The upper limit is found when photogenerated carriers are distributed homogeneously over the whole mesa. In this situation, the ratio between both IV curves is equal to the ratio between the area of the mesa and the area of the excitation spot. That would be the case for the 1J solar cell (Fig. 2c) where the EL- and PL-based curves differ by a factor of 4 at all voltages, identical to the ratio of the areas. Conversely, low conductivity will reduce the in-plane transport and therefore the EL- and PL-based curves will be similar, at least at high injection. This is the trend observed in all other cases.

It should be noted that this argument can be applied also to the EL: a poor conductivity will mean that the injected region is not the whole mesa, as we have assumed, but a smaller area, and therefore, we will be over- or under-

estimating overestimating the current injected in the collection region, depending on the specific grid design. That could be the case for the GaInP subcell in the 2J solar cell. This situation is often observed in solar cells with high sheet resistance.

This comparison between the EL- and PL-based IV curves, together with a more elaborate model that the one of Fig. 7a, could allow for a very fast characterisation of the in-plane conductivities of the materials on standard, fully processed solar cells, giving information about their quality, their performance under inhomogenous illumination conditions or the quality of the design of the metal grid.

As a stand-alone characterisation technique, however, it will be necessary to minimise the in-plane transport of photogenerated carriers in order to have a reliable PL-based IV curve. This means that the excitation spot must cover the whole sample – the mesa, in the case of devices – situation where it might difficult to achieve homogeneous illumination or even enough injected current in the case of very large areas, common in silicon-based solar cells.

It should be noted that the method does not involve taking images of the sample, such as in [5] or [6] and therefore it is expected to be much faster, more sensitive, computationally less intensive and cheaper, therefore more suitable for a manufacturing environment.

## 5.2 Speed and accuracy

All the results presented in Fig. 2, 3 and 5 support the claim that internal voltages of a MJ solar cell can be accurately estimated using a contactless and fast characterisation tool, as it is PL. In our case, each point in the IV curves takes <100 ms to be measured, meaning that with a correct automation and exciting simultaneously with all lasers, the complete IV of all subcells in a MJ solar cell could be measured in a matter of 1-2 s, depending on the desired resolution.

Once the implied IV curves are known, solar cell parameters such as the saturation currents associated to  $n=1$  and  $n=2$  ideality factors or the  $V_{oc}$  and the FF at any injection level could be estimated for each subcell. In the case of the 6J solar cell, at 200 Suns (see Fig. 5), the  $V_{oc}$  would be: 1.14V, 1.22V, 1.46V and 1.64V for the GaInAs, AlGaInAs, GaInP and AlGaInP subcells, respectively.

For the voltages, the accuracy of the method depends on the accuracy of the measured  $Q_e$ , the luminescence and the temperature, as well as the calibration factor. While a 10% relative error in the  $Q_e$  or the luminescence only produces an absolute change in the voltage of around 2.6mV each at room temperature, according to Eq. 2, the noise in the signal, the influence of the background, the tail of the laser and temperature drift with power increases that uncertainty, specially for low luminescence intensities.

In the end, the latter is the main limitation of the method, shared with the EL-based IV curves: the solar cells have to emit enough light, meaning that poor quality materials or low injection conditions can not be measured with low sensitivity setups.

## 6 CONCLUSIONS

In this work we have presented a PL-based IV characterization method for MJ solar cells that allows for a fast, contactless measurement applicable even in unfinished devices. Results have been presented for 1J, 2J

and 6J devices. At high injection conditions, the PL-based IV curves overlap to those obtained from EL measurements and normal dark IV measurements. At low injection, however, currents are overestimated in the PL experiments. We attribute this to in-plane carrier transport from the region under illumination to the region in the dark.

Despite this drawback, that can be solved by using a larger illumination area, the results support the validity of the technique as a characterization tool able of fast screening the internal IV curves of an arbitrary number of subcells in a MJ device.

## 7 REFERENCES

- [1] T. Trupke, R. a. Bardos, M. D. Abbott, and J. E. Cotter, *Appl. Phys. Lett.*, vol. 87, no. 2005, pp. 2013–2016, 2005.
- [2] L. Lombez, M. Paire, A. Delamarre, G. El-hajje, D. Ory, D. Lincot, and F. Guillemoles, *2014 IEEE 40th Photovoltaic Specialist Conference (PVSC)*, 2014, 1–3.
- [3] T. Kirchartz, U. Rau, M. Hermle, A. W. Bett, A. Helbig, and J. H. Werner, *Appl. Phys. Lett.*, vol. 92, no. 2008, pp. 90–93, 2008.
- [4] S. Philipps, W. Guter, E. Welsler, J. Schöne, M. Steiner, F. Dimroth, and A. Bett, Chapter 1 in *Next Generation of Photovoltaics SE - 1*, vol. 165, A. B. Cristóbal López, A. Martí Vega, and A. Luque López, Eds. Springer Berlin Heidelberg, 2012, pp. 1–21.
- [5] H. Hoffler, O. Breitenstein, and J. Haunschild, *IEEE J. Photovoltaics*, vol. 5, no. 2, pp. 613–618, Mar. 2015, and references therein.
- [6] A. Delamarre, L. Lombez, and J. F. Guillemoles, *Appl. Phys. Lett.*, vol. 100, no. 2012, pp. 17–20, 2012.

## 8 ACKNOWLEDGEMENTS

We acknowledge the financial support from the EMRP Researcher Grant Contract NO. ENG51-REG3. EMRP is jointly funded by the EMRP participating countries within EURAMET and the European Union.